Computer Simulation of Staphylococcal Nuclease Action on Thymidine 3′,5′-Bis(phosphate) (pdTp)[1]

Joan A. Deiters,[1a] Judith C. Gallucci, and Robert R. Holmes*

Contribution from the Department of Chemistry, University of Massachusetts, Amherst, Massachusetts 01003. *Received February 23, 1981*

Abstract: Computer modeling based on a molecular mechanics approach was used to explore the mechanism of staphylococcal nuclease action on the thymidine 3′-phosphate 5′-(*p*-nitrophenyl phosphate)–calcium ion substrate complex. The active-site residues Asp-21, Asp-40, Glu-43, Arg-35, Tyr-113, Lys-84, Arg-87, and Tyr-85 were included in the calculation. Initially the X-ray coordinates were used for the enzyme active-site residues with the inhibitor substrate, thymidine 3′,5′-bis(phosphate) (pdTp), in place. Subsequently, introduction of the *p*-nitrophenyl group and energy minimization gave the coordinates for the active substrate. In-line attack by hydroxide was simulated by approach opposite the phosphoryl oxygen atom attached to the *p*-nitrophenyl group (path 1) and by approach opposite the phosphoryl oxygen atom attached to thymidine (path 2). The former pathway is the route that leads to products observed in nonenzymatic cleavage. The latter pathway is the enzymatic route. Computer simulation of the hydrolysis reaction under enzyme constraints shows that path 2 is of significantly lower energy, in agreement with the observed enzyme action. Simulation in the absence of enzyme constraints results in similar energies for the two pathways. Since the *p*-nitrophenyl group is the better leaving group, the expected products in nonenzymatic hydrolysis are those observed experimentally, nitrophenoxide ion and thymidine 3′,5′-phosphate. Adjacent attack accompanied by pseudorotation is not felt to be a viable enzymatic route.

Inferences about enzyme mechanisms have enjoyed the most credibility when supported by single-crystal X-ray diffraction[2] studies or by NMR investigations[3] employing paramagnetic probes resulting in detailed structural information on active-site–substrate complexes. For the ribonuclease–uridylyl-(3′,5′)-adenosine (UpA) system, we have found[4] that computer modeling based on a molecular mechanics approach serves as a useful probe in exploring the relative energy profiles for possible mechanistic variations. By use of X-ray coordinates to initiate the computer simulation, a low-energy in-line attack leading to a cyclic intermediate via a pentacoordinated transition state was obtained.[4] The result was in essential agreement with findings based on physical and chemical studies for the first step of RNase action.[5]

In this paper, we carry out a similar computer simulation to obtain a reaction pathway for the hydrolysis of the active substrate, thymidine 3′-phosphate 5′-(*p*-nitrophenyl phosphate) (*p*-NO_2Ph–pdTp), by the staphylococcal nuclease–calcium ion enzyme system.

The mechanism of action of RNase and staphylococcal nuclease is quite different.[5-7] While both hydrolyze nucleic acids to produce 3′-nucleoside monophosphates via a proposed trigonal-bipyramidal transition state, RNase acts only on RNA fragments, but staphylococcal nuclease acts on both RNA and DNA units. The fact that staphylococcal nuclease does not hydrolyze 2′,3′-cyclic phosphate esters is consistent with the lack of evidence suggesting that staphylococcal nuclease proceeds through cyclic phosphate intermediates like that supported for the first step of RNase action.

An interesting feature of the hydrolysis of *p*-NO_2Ph–pdTp by staphylococcal nuclease is the exclusive formation of *p*-nitrophenyl phosphate[8] caused by cleavage of the poorer leaving group, the 5′-oxyanion of thymidine. In nonenzymatic base hydrolysis of the same substrate, displacement of the better leaving group, nitrophenoxide, takes place. Within the framework of established principles of pentacoordination,[9] these results are consistent with in-line attack,[10] as expressed in Figure 1 by path 1 for nonenzymatic hydrolysis and by path 2 for enzymatic action. Apparently, active-site enzyme constraints are responsible in causing a changeover in mechanism from what might be expected to be the preferred mechanism.

Considerable structural information is at hand on staphylococcal nuclease to support an in-line mechanism leading to a pentacoordinate transition state of the type implied by path 2.[11] The crystal structure determined to 2-Å resolution[2d,12,13] for the nuclease–thymidine 3′,5′-bis(phosphate) (pdTp)–calcium ion complex indicates the 5′-phosphate oriented for possible incipient nucleophilic attack. Incisive NMR studies involving pdTp[14,15] implicate Tyr-85 and Tyr-113 at the active site. Active-site interactions have been further characterized by use of paramagnetic relaxation techniques on the related nuclease–pdTp–Gd(III) complex.[3a] The above structural evidence has been correlated with inferences from chemical studies to give the mechanism summarized in Figure 2.[15]

There appears to be sufficient room between the Ca(II) ion and the 5′-phosphorus atom to accommodate an intervening water molecule or hydroxyl group that might be responsible for in-line nucleophilic attack.[16,17] The presence of Arg-35 and Arg-87, hydrogen-bonded to the phosphoryl oxygens, favors an S_N2 mechanism by electron withdrawal at phosphorus. The presence of the coordinated Ca(II) ion favors an S_N2 mechanism by enhancement of the nucleophilicity of the attacking water mole-

(1) (a) Department of Chemistry, Vassar College, Poughkeepsie, NY. (b) Pentacoordinated Molecules. Part 41. For Part 40, see: Richman, J. E.; Day, R. O.; Holmes, R. R. *Inorg. Chem.* **1981**, *20*, 3378.

(2) (a) Sweet, R. M.; Wright, H. T.; Janin, J.; Chothia, C. H.; Blow, D. M. *Biochemistry* **1974**, *13*, 4212. (b) Huber, R.; Kukla, D.; Bode, W.; Schwager, P.; Bartels, K.; Deisenhofer, J.; Steigemann, W. *J. Mol. Biol.* **1974**, *89*, 73. (c) Huber, R.; Bode, W.; Kukla, D.; Kohl, U.; Ryan, C. A. *Biophys. Struct. Mech.* **1975**, *1*, 189. (d) Cotton, F. A.; Hazen, E. E., Jr. *Enzymes, 3rd ed.*, **1971**, *4*, 153–174.

(3) (a) Furie, B.; Griffen, J. H.; Feldmann, R. J.; Sokoloski, A.; Schechter, A. N. *Proc. Natl. Acad. Sci. U.S.A.* **1974**, *71*, 2833. (b) Mildvan, A. S. *Acc. Chem. Res.* **1977**, *10*, 246. (c) Mildvan, A. S.; Cohn, M. *Adv. Enzymol. Related Areas Mol. Biol.* **1970**, *33*, 1.

(4) Holmes, R. R.; Deiters, J. A.; Gallucci, J. C. *J. Am. Chem. Soc.* **1978**, *100*, 7393.

(5) For a more extensive coverage than ref 4, see: Holmes, R. R. "Pentacoordinated Phosphorus", Americal Chemical Society: Washington, DC, 1980; Vol. II, ACS Monogr. No. 176.

(6) Richards, F. M.; Wyckoff, H. R. *Enzymes, 3rd Ed.*; **1971**, *4*, 647–806.

(7) Anfinsen, C. B.; Cuatrecasas, P.; Taniuchi, H. *Enzymes, 3rd Ed.* **1971**, *4*, 177–204.

(8) Dunn, B. M., DiBello, C.; Anfinsen, C. B. *J. Biol. Chem.* **1973**, *248*, 4769.

(9) Holmes, R. R. "Pentacoordinated Phosphorus"; American Chemical Society: Washington, D.C., 1980; Vol. I, ACS Monogr. No. 175.

(10) Reference 5, p 181.

(11) For recent reviews, see: (a) Reference 5, p 213 ff. (b) Tucker, P. W.; Hazen, E. E., Jr.; Cotton, F. A. *Mol. Cell. Biochem.* **1978**, *22*, 67; **1979**, *23*, 3, 67, 131.

(12) Arnone, A.; Bier, C. J.; Cotton, F. A.; Day, V. W.; Hazen, E. E., Jr.; Richardson, D. C.; Richardson, J. S.; Yonath, A. *J. Biol. Chem.* **1971**, *246*, 2302.

(13) Protein Data Bank, Department of Chemistry, Brookhaven National Laboratory, Upton, NY.

(14) Markley, J. L.; Jardetzky, O. *J. Mol. Biol.* **1970**, *50*, 223.

(15) Roberts, G. C. K.; Jardetzky, O. *Adv. Prot. Chem.* **1970**, *24*, 447.

(16) Mildvan, A. S.; Grisham, C. M. *Struct. Bonding (Berlin)* **1974**, *20*, 1.

(17) Mildvan, A. S. *Annu. Rev. Biochem.* **1974**, *43*, 357.

0002-7863/82/1504-5457$01.25/0

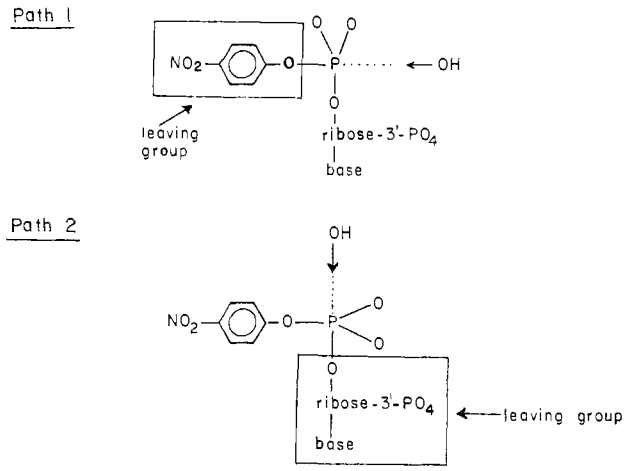

Figure 1. Alternate pathways for nonenzymatic and enzymatic hydrolysis of *p*-NO_2Ph–pdTp. Path 1 leads to products observed in nonenzymatic hydrolysis and path 2 to products observed in enzymatic hydrolysis by staphylococcal nuclease.

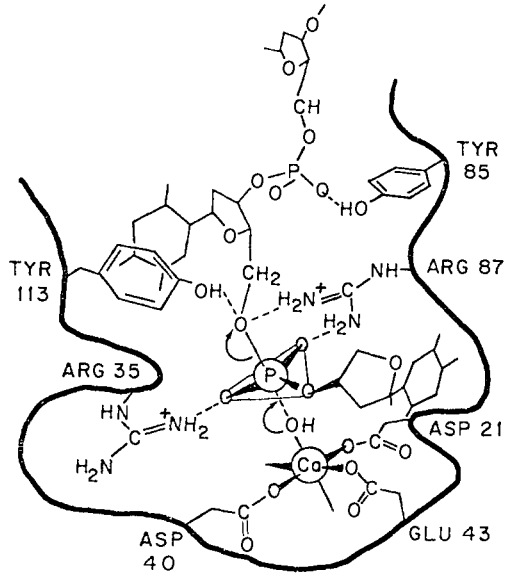

Figure 2. Possible mechanism for hydrolysis of a polynucleotide by staphylococcal nuclease.

cule.[16,17] Recently, the crystal structure data on the nuclease–pdTp–Ca(II) ion system has been refined to 1.5 Å.[18] These results suggest that a water molecule bound between Glu-43 and an oxygen atom of the 5′-phosphate may be responsible for initiating the in-line attack by proton transfer to Glu-43.

In modeling staphylococcal nuclease action on the active substrate, *p*-NO_2Ph–pdTp, using techniques devised for a molecular mechanics approach to the ribonuclease–UpA system,[4,19] we chose as a starting point the 2-Å resolution data[13] on the nuclease–pdTp–Ca(II) ion system. After introduction of enzyme constraints and conformational minimization, the substrate is altered to the active derivative, *p*-NO_2Ph–pdTp, and energy minimization once again is performed. Feasible reaction pathways are explored then to obtain low-energy profiles with and without enzyme constraints to ascertain possible features influencing the change in hydrolysis mechanism encountered on going from the enzyme to the nonenzyme system. Lastly, consideration of the effects of use of the higher resolution X-ray data[18] is discussed.

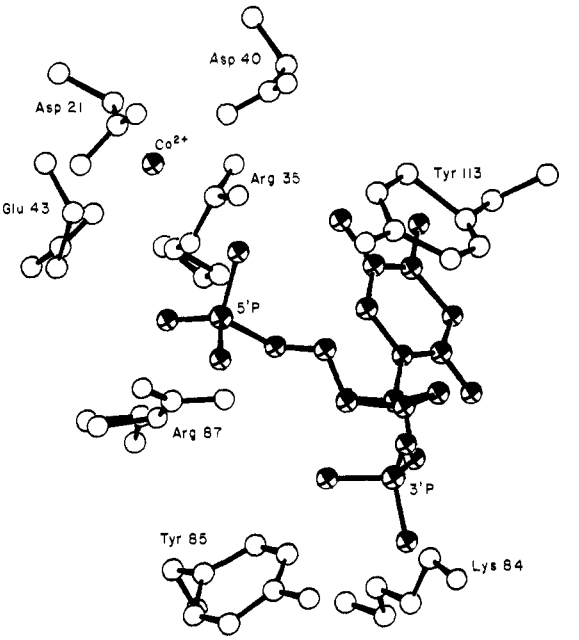

Figure 3. ORTEP drawing of pdTp in the enzyme active site of staphylococcal nuclease. Atom positions are obtained from 2.0-Å X-ray data.[13] Open circles designate atoms of the enzyme active site, and shaded circles designate atoms of the pdTp substrate.

Table I. Calculated Energy of Staphylococcal Nuclease-pdTp-Ca(II) Ion System[a]

	atomic coordinates from X-ray data[b]	atomic coordinates of min energy conformation[c]
ΣE_{str}[d]	582.90	0.79
ΣE_{bend}	43.22	3.27
ΣE_{VDW}[e]	0.82	−3.64
ΣE_{tors}	5.98	0.18
ΣE_{steric}	632.92	0.60

[a] All energies are reported in kcal/mol. [b] No hydrogen atoms were included in calculations of energy terms. [c] Hydrogen atoms were included in calculation of energy terms. [d] See eq 1 for definition of energy terms. [e] $\Sigma E_{VDW} = \Sigma E_{nB} + \Sigma E_{EPR}$.

In application of the molecular mechanics method,[20] the energy for a molecule is calculated as a sum of several potential functions:

$$E_{steric} = \Sigma E_{str} + \Sigma E_{bend} + \Sigma E_{tors} + \Sigma E_{nB} + \Sigma E_{EPR} \quad (1)$$

The stretch and bend terms are modified Hooke's law expressions; E_{tors} is the torsional-energy contribution computed by a cosine law; E_{nB} includes van der Waals interactions between atoms not bonded to a common atom; and E_{EPR} is a term for energy of repulsion between atoms bonded directly to phosphorus, due to their electron-pair interactions.[19a] The last term was introduced to obtain good agreement between calculated and experimentally determined structures for the phosphoranes. For each term, the sum is over all interactions for the molecule, and the total energy is minimized with respect to all positional coordinates.

Initial Minimum Energy for the Enzyme Inhibitor Complex. For initialization of the model calculation, all atomic coordinates for the non-hydrogen atoms of the inhibitor molecule, pdTp, and the calcium ion were used along with atomic coordinates for the residues involved at the active-site region of staphylococcal nuclease: Asp-21, Asp-40, Glu-43, Arg-35, Arg-87, Tyr-113, Tyr-85, and Lys-84. These initial coordinates, available from the 2-Å X-ray study,[13] are shown in Figure 3.

(18) Cotton, F. A.; Hazen, E. E., Jr.; Legg, M. J. *Proc. Natl. Acad. Sci. U.S.A.* **1979**, *76*, 2551, and personal communication from E. E. Hazen, Jr.

(19) The program we developed for nonrigid phosphorus compounds [(a) Deiters, J. A.; Gallucci, J. C.; Clark, T. E.; Holmes, R. R. *J. Am. Chem. Soc.* **1977**, *99*, 5461] is an extension of the molecular mechanics program of Allinger et al. [(b) Allinger, N. L.; Tribble, M. T.; Miller, M. A.; Wertz, D. H. *Ibid.* **1971**, *93*, 1637. Wertz, D. H.; Allinger, N. L. *Tetrahedron* **1974**, *30*, 1579].

(20) The calculational methods of conformation analyses have been reviewed by Williams et al. (Williams, J. E.; Stang, P. J.; Schleyer, P. v. R. *Annu. Rev. Phys. Chem.* **1968**, *19*, 531.

Table II. Staphylococcal Nuclease-pdTp-Ca(II) Ion Interactions Included in the Calculation

interaction	atom nos[a]	interatomic dist,[b] Å	l_o,[c] Å	k_s,[c] mdyne/Å
Ca^{2+}-Asp-21[d]	Ca(26)-O(45)	2.4	2.5	0.1
Ca^{2+}-Asp-40	Ca(26)-O(50)	2.3	2.5	0.1
Ca^{2+}-Glu-43	Ca(26)-O(56)	2.9	2.5	0.1
Arg-35-5′-phosphate	N(62)-O(24)	2.9	2.9	0.1
Arg-35-5′-phosphate	N(65)-O(23)	2.1	2.9	0.1
Arg-87-5′-phosphate	N(73)-O(21)	2.9	2.9	0.1
Arg-87-5′-phosphate	N(72)-O(24)	2.7	2.9	0.1
Lys-84-3′-phosphate	N(97)-O(20)	2.9	3.0	0.05
Tyr-85-3′-phosphate	O(91)-O(20)	3.1	3.0	0.05

[a] Refer to numbering scheme in Figure 4 and interactions depicted in Figure 5. [b] Distance calculated from X-ray coordinates.[13] [c] The parameter l_o is the "strainless" value for bond length; k_s is the stretching force constant for the bond. [d] A weak bending force constant was applied to the O-Ca-O bonds to maintain octahedral geometry around the calcium ion.

For energy minimization using molecular mechanics, "strainless" bond lengths, bond angles, force constants, and torsional parameters are needed. Bond lengths, l_o, and force constants, k_s, were Allinger's values[19b] or bond lengths from X-ray structure of thymidine[21] with k_s values calculated by Badger's rule.[22] "Strainless" angles, α_o, and force constants, k_b, were Allinger's values[19b] or values from the thymidine structure.[21] Torsional constants were used to maintain planarity of the base plane, and 1,3 interactions were used at both phosphorus atoms with the value of D set at 0.1.[4,19a]

After computation of an initial energy (Table I), a geometry search under the above constraints led to a minimum energy conformation. The latter conformation was an intermediate point that expedited the completion of the parameterization. Next hydrogen atoms were added to the pdTp substrate of this intermediate conformation, bringing the atom total to 97.

In later calculations dealing with the reaction pathway, hydrogen atoms were selectively added to enzyme residues where steric hindrance was apparent. Since their addition caused an insignificant effect on the barrier height of the transition state in the enzymatic system for both path 1 and path 2 and our calculated starting conformation without their inclusion corresponded closely to the conformation resulting from X-ray analysis, we felt their omission in the formation of the active substrate and reaction coordinates would produce no serious effect and have the positive effect of reducing the complexity of the calculations.

The following set of conditions was imposed on the system during the subsequent energy minimization to mimic enzyme constraints: (1) The angle between thymine base plane and a plane through three atoms of ribose was held constant. (2) The α-carbons of each amino acid moiety were held fixed during energy minimization. (3) Weak interactions between substrate and enzyme were introduced. The latter interactions are discussed next.

The initial X-ray coordinates for the system pdTp–enzyme–Ca(II) ion were searched for interatomic distances of 3.0 Å or less that might indicate enzyme–substrate interactions. The nine interactions selected, based on close proximity of the atoms and suggestions in the literature,[2d,23,24] are shown in Table II along with the l_o and k_s values used for the interactions in the energy minimization. See Figure 4 for the numbering system used to identify the atoms. Figure 5 indicates the nine interactions of Table II included in the calculation. The conventional numbering

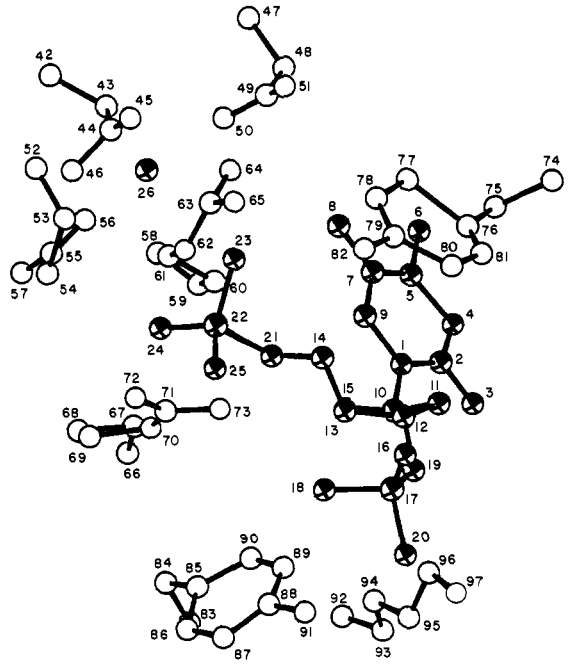

Figure 4. Numbering scheme used for energy minimization for all calculations. For p-NO_2Ph–pdTp, the p-nitrophenyl group is added to O_{25} of 5′-phosphate. For calculations on the isolated p-NO_2Ph–pdTp system, the atoms corresponding to the enzyme fragments are omitted. Open circles designate atoms of the enzyme active site, and shaded circles designate atoms of the substrate.

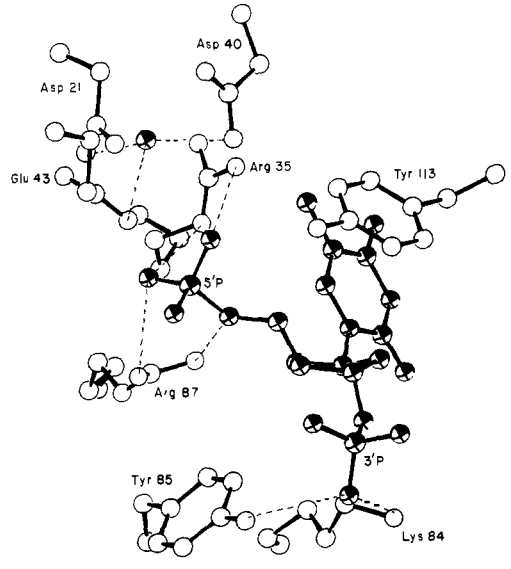

Figure 5. ORTEP drawing of pdTp in the staphylococcal nuclease active site based on coordinates obtained from energy minimization. Open circles designate atoms of the enzyme and shaded circles designate atoms of the pdTp substrate. Dotted lines show enzyme–substrate interactions included in the calculation (same orientation as Figure 3). Hydrogen atoms of the substrate are not shown in the drawing but were included in calculation of the minimum energy conformation.

system for pdTp is shown in Figure 6. The interaction of calcium ion with the carboxylate side chains of Asp-21, Asp-40, and Glu-43 is suggested by Cotton and Hazen on the basis of the 2-Å X-ray structure.[2d] They also propose possible hydrogen-bond interactions of the 3′-phosphate group with the phenolic hydroxyl group of Tyr-85 and the ϵ-amino group of Lys-84. The hydrogen-bonding interaction of Arg-35 and Arg-87 with the 5′-phosphate was also proposed by them[2d] and further explored in an X-ray study of a simpler model for the interaction.[23,24] In all calculations on the enzyme–substrate complex, weak force constants were applied to maintain the close proximity of the atoms involved in the interactions.

(21) Young, D. W.; Tollin, P.; Wilson, H. R. *Acta Crystallogr., Sect B* **1969**, *B25*, 1423.
(22) Badger, R. M. *J. Chem. Phys.* **1935**, *3*, 710; **1934**, *2*, 128.
(23) Cotton, F. A.; Day, V. W.; Hazen, E. E., Jr.; Larsen, S. *J. Am. Chem. Soc.* **1973**, *95*, 4834.
(24) (a) Cotton, F. A.; Hazen, E. E., Jr.; Day, V. W.; Larsen, S.; Norman, J. G.; Wong, S. T. K.; Johnson, K. H. *J. Am. Chem. Soc.* **1973**, *95*, 2367. (b) Cotton, F. A.; Day, V. W.; Hazen, E. E., Jr.; Larsen, S.; Wong, S. T. K. *Ibid.* **1974**, *96*, 4471.

Table III. Comparison of Conformational Parameters Obtained from X-Ray Data and from Minimum Energy Calculations

	enzyme system			nonenzyme system		
	X-ray[13] conformation	min energy pdTp (calcd)	min energy p-NO_2Ph-pdTp (calcd)	X-ray[26] conformation	min energy pdTp (calcd)	min energy p-NO_2Ph-pdTp (calcd)
			Dihedral Angle (Deg)			
thymine-ribose planes[a]	66.0	67.5	64.5	81.5	83.8	83.0
$\phi_{C-N}(O'_1C_1N_1C_2)$	−18.8 (anti)	−24.0 (anti)	−23.8 (anti)	−43.3 (anti)	−39.2 (anti)	−32.4 (anti)
$\phi_{O-O}(O'_5C'_5C'_4O'_1)$	56.3	54.0	56.5	62.7	44.8	45.6
$\phi_{O-C}(O'_5C'_5C'_4C'_3)$	171.1	173.6	176.0	57.2	72.8	71.8
			Distance (Å) from Mean Plane 1[c]			
C_2'	−0.33	−0.37	−0.34	0.40	0.26	0.35
C_5'	−1.31	−1.21	−1.18	−0.71	−0.68	−0.66
N	−1.11	−1.01	−1.00	−1.15	−1.08	−1.05
O_3'	1.27	1.31	1.28	0.61	0.61	0.63
			Distance from Mean Plane 2[d]			
C_3'	0.27	0.32	0.26	−0.53	−0.43	−0.47
C_5'	−1.31	−1.22	−1.20	−0.72	−0.75	−0.69
N	−1.09	−0.99	−0.96	−1.11	−1.00	−1.00
O_3'	1.61	1.70	1.61	−0.13	0.02	−0.08
			Designation of Sugar Conformation			
	C_2' endo (Figure 3)	C_2' endo (Figure 5)	C_2' endo (Figure 7)	C_3 endo (Figure 11)	C_3 endo	C_3 endo (Figure 12)

[a] Five atoms included in ribose plane. [b] All atom numbers refer to scheme used in Figure 6. [c] Ribose plane without C_2'. [d] Ribose plane without C_3'.

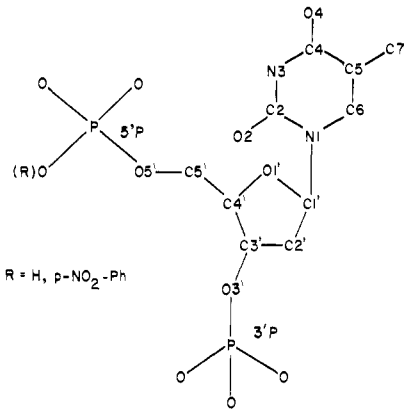

Figure 6. Conventional numbering scheme for pdTp and p-NO_2Ph-pdTp.

Table I shows the total energy and the breakdown in the energy terms making up eq 1 for the initial conformation and the minimum energy conformation. The high strain energy based on the initial set of coordinates is due to the uncertainity in the atomic positions in the 2.0-Å X-ray study[2d,12] and to the choice of "strainless" bond parameters. The minimum energy pdTp–enzyme–Ca(II) ion conformation is shown in Figure 5. In Table III and in a comparison of Figures 3 and 5, it can be seen that the energy minimization does not affect the conformation of the pdTp, but does involve some changes in the positions of the enzyme residues. It is interesting to note that the greatest changes occur in the area around the calcium ion. This is the area that shows also the greatest change in X-ray data when 2.0-Å data are compared with 1.5-Å data.[11b]

Conversion of pdTp to an Active Enzyme–Substrate Complex. Since pdTp is an inhibitor of staphylococcal nuclease activity, it is necessary to modify the substrate in order to have a model of an active complex for hydrolysis reaction. The addition of a p-nitrophenyl group to the 5'-phosphate of pdTp converts the inhibitor to an active substrate.[25] We assumed that phenyl ring addition would not greatly alter the thymidine conformation and that the phenyl ring would be added to the phosphate oxygen that was not involved in hydrogen bonding, i.e., O_{25}. To keep within the program limit of 100 atoms, we replaced some atoms that seemed to be only indirectly involved in enzyme reaction by p-nitrophenyl atoms.

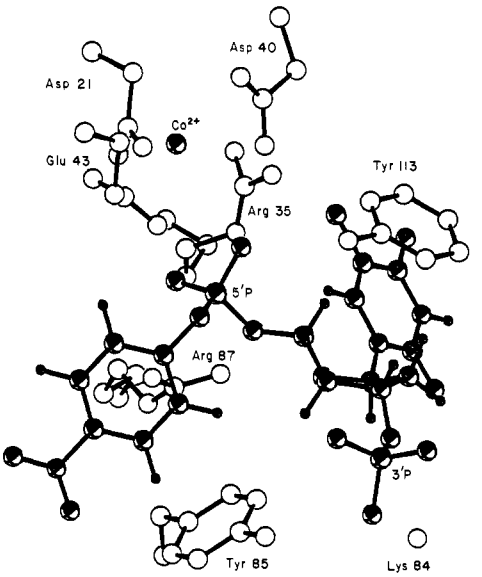

Figure 7. ORTEP drawing of p-nitrophenyl pdTp in the staphylococcal nuclease active site based on coordinates obtained from energy minimization. Open circles designate atoms of enzyme; shaded circles, atoms of substrate (same orientation as Figure 3).

It was necessary to rotate the phenyl ring in 20° increments about the $P-O_{25}$ bond and minimize the geometry at each of these points. This rotation followed by minimization was necessary because rotation about the P–O bond sweeps the phenyl ring through a large volume of space and the computer minimization techniques do not move the atoms sufficiently to achieve the lowest possible energy. A conformation with a torsional angle of 77° ($O_{21}P_{22}O_{25}C_{Ph}$) was found to have the lowest energy conformation. The phenyl ring was then rotated about the O_{25}–phenyl bond. Here, it really was not necessary to rotate and then minimize each geometry because the phenyl ring could easily slip into its minimum energy conformation with a torsional angle ($P_{22}-O_{25}-C_{Ph}-C_{Ph}$) of approximately 90°.

The structure of the minimum energy conformation of p-NO_2Ph–pdTp in the enzyme site is shown in Figure 7 and some

(25) Cuatrecasas, P.; Wilchek, M.; Anfinsen, C. B. *Biochemistry* **1969**, *8*, 2277.

Table IV. Bond Parameters for Attacking and Leaving Groups at Points along Reaction Pathways

	1	2	3	4	5	6	7	8	9	10
					P-OH[a] Bond					
l_o[b]	3.5	3.0	2.5	2.0	1.9	1.8	1.78	1.7	1.6	1.59
k_s[c]	0.00	0.18	0.41	1.18	1.56	2.10	2.2	2.91	4.22	4.4
					P-OR[d] Bond					
l_o	1.59	1.60	1.61	1.67	1.71	1.77	1.78	1.92	3.00	3.5
k_s	4.40	4.22	3.99	3.22	2.84	2.30	2.20	1.49	0.18	0.00
					Sum of k_s Values for P-OH and P-OR Bonds					
	4.40	4.40	4.40	4.40	4.40	4.40	4.40	4.40	4.40	4.40

[a] P-OH bond is the P-O bond formed by attacking group. [b] l_o values are the "strainless" bond lengths (Å). [c] k_s values are the bond stretching force constants (mdyne/Å). [d] P-OR bond is the P-O bond of the leaving group.

conformational parameters for the substrate are given in Table III for comparison to X-ray data. The conformation of the substrate has not been drastically altered by the minimization process (cf. Figure 7 with Figures 5 or 3).

Conditions Imposed on the Reaction Pathway Calculations. Having established a minimum energy structure for an active substrate–enzyme complex, it is necessary to define conditions under which the enzyme hydrolysis reactions will be simulated. As described in Figure 1, path 1 refers to in-line attack by the OH group opposite the phosphate oxygen atom attached to the phenyl ring (O_{25} in the numbering scheme of Figure 4) and path 2 refers to in-line OH attack opposite the phosphate oxygen atom attached to the 5′-carbon of the nucleotide (O_{21} of Figure 4). The latter is the experimentally observed enzymatic pathway.[8,25]

For all angles in which phosphorus is the central atom, the bending force constant was set at zero. This implies that there is no one ideal "strainless" geometry to which phosphorus is constrained and allows the phosphorus geometry to be determined solely by nonbonded interactions and by electron pair repulsion terms.[19a] There was, however, one angle which was an exception to this condition. The O–P–O angle formed by the attacking and leaving oxygen atoms was held at 180° by applying a force constant of 1.0 [(mdyn Å)/rad^2].

Minimum energy conformations were calculated at 10 points along the reaction coordinate. The only paarameters that varied from one point to the next were the "strainless" bond lengths (l_o) and stretching force constants (k_s) for the attacking and leaving groups. At each point a "strainless" P–O bond length, l_o, was selected for the attacking group. From this bond length, the corresponding force constant, k_s, was calculated by using Badger's rule.[22] The force constant of the leavhing group (i.e., the group that is 180° from the attacking group) was selected so that the sum of the two force constants for the entering and leaving group was constant. A value of 4.4 was used for this constant.

$$k_s(\text{P–OH})_{\text{attacking}} + k_s(\text{P–OR})_{\text{leaving}} = \text{constant} \qquad (2)$$

The set of l_o and k_s parameters used for all pathways is given in Table IV.

The reason for using eq 2 is that it provides a method whereby a rapid change in the long bond is accompanied by a small change in the shorter bond. This leads to a fairly smooth energy path that reaches maximum energy at the transition state where k_s(P–OH) = k_s(P–OR). Also the length of the P–O_{axial} bonds, ~1.8 Å, in the transition state is reasonable.[9] The minimum energy conformation calculated at one point was used as a starting geometry for the next point. Thus, the reaction was simulated by a movement of atoms along the reaction pathway.

Enzyme Hydrolysis. By use of the latter conditions defining the way that the reaction pathway is to be calculated for the enzymatic hydrolysis and application of the enzyme constraints discussed earlier, an energy–structure profile was obtained for the two pathways of Figure 1. The results are listed in Tables V (path 1) and VI (path 2). The comparative energy profile is shown in Figure 8. ORTEP plots of the transition-state structures for paths 1 and 2 are presented in Figures 9 and 10, respectively.

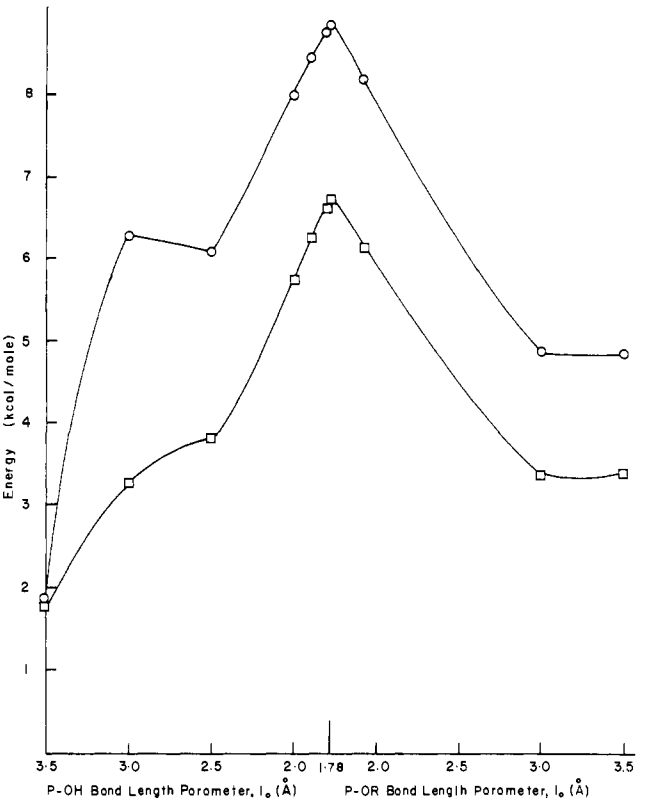

Figure 8. Energy profile for two alternate modes of hydrolysis of *p*-NO_2Ph–pdTp in the staphylococcal nuclease environment. Circles indicate path 1; squares, path 2. See Figure 1 for definition of pathways. The attacking group is OH and leaving group is OR (R = O_{25}–Ph in path 1 and O_{21}–ribose in path 2). Experimentally, path 2 is the preferred path in enzymatic hydrolysis.

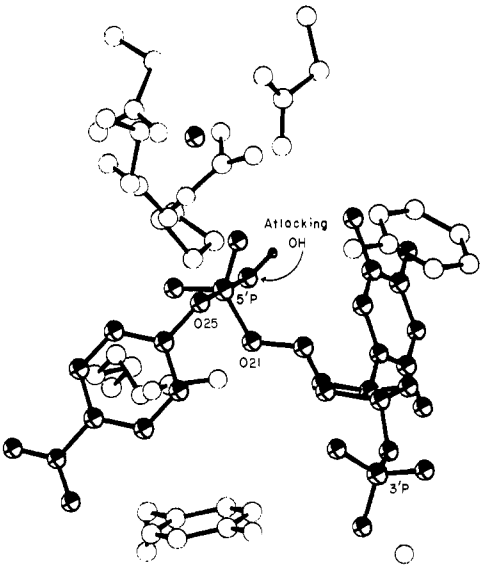

Figure 9. ORTEP drawing of path 1 transition state in hydrolysis of *p*-NO_2Ph–pdTp in the staphylococcal nuclease environment. Attacking OH is opposite O_{25}–Ph (See Figure 1). Phosphorus bond angles for the transition state are given in Table V, column 7. Open circles designate atoms of enzyme; shaded circles, atoms of *p*-NO_2Ph–pdTp substrate. Path 1 is of higher energy than path 2 in enzyme environment. Orientation of drawing is same as Figure 3.

Cleavage in Nonenzymatic Environment. To obtain comparative data on the pathways for hydrolysis in Figure 1 for nonenzymatic hydrolysis with the same substrate, we used the X-ray coordinates determined for calcium thymidylate by Trueblood et al. as starting coordinates.[26] These are projected in Figure 11.

Table V. Reaction Path 1 for p-NO_2Ph–pdTp Enzyme System (Attacking Group Is OH; Leaving Group Is O_{25}[a])

	point on pathway[b]									
	1	2	3	4	5	6	7[c]	8	9	10
					Bond Length, Å					
P-OH	8.26	2.95	2.54	2.05	1.94	1.83	1.81	1.72	1.61	1.60
$P-O_{25}$	1.60	1.61	1.62	1.69	1.74	1.80	1.82	1.96	2.98	2.96
$P-O_{21}$	1.60	1.60	1.60	1.60	1.60	1.60	1.60	1.60	1.60	1.60
$P-O_{23}$	1.50	1.50	1.50	1.50	1.50	1.50	1.50	1.50	1.50	1.50
$P-O_{24}$	1.50	1.50	1.50	1.50	1.50	1.50	1.50	1.50	1.50	1.50
					Angle, deg					
$O_{21}PO_{23}$	111.0	116.4	121.9	129.5	131.0	132.4	132.6	132.4	121.9	122.2
$O_{21}PO_{24}$	109.2	104.6	108.4	113.9	114.6	115.0	115.0	114.6	104.4	104.4
$O_{21}PO_{25}$	108.9	111.7	107.9	99.9	97.6	94.8	94.3	90.8	76.9	76.9
O_{21}-P-OH	71.3	67.7	71.5	79.2	81.5	84.1	84.6	88.1	102.1	102.2
$O_{23}PO_{24}$	108.4	108.6	110.5	112.5	112.5	112.4	112.2	112.5	109.8	109.6
$O_{23}PO_{25}$	106.5	104.9	100.0	90.1	87.7	84.9	84.5	81.0	68.6	68.7
O_{23}-P-OH	74.1	75.4	80.6	90.2	92.7	95.5	96.0	99.5	111.6	111.6
$O_{24}PO_{25}$	112.9	110.7	107.4	100.7	98.7	96.3	95.8	92.3	75.1	75.1
O_{24}P-OH	66.4	69.6	73.1	80.0	82.0	84.5	84.9	88.5	105.7	105.7
O_{25}P-OH	179.2	179.4	179.3	179.1	179.0	178.9	178.9	178.8	178.9	178.9
					Energy, kcal/mol					
ΣE_{str}	1.01	0.91	0.97	1.25	1.28	1.30	1.31	1.22	0.89	0.89
ΣE_{bend}	3.43	3.78	3.60	3.60	3.63	3.64	3.65	3.60	3.59	3.58
ΣE_{VDW}[d]	−2.73	0.49	0.99	2.92	3.34	3.65	3.71	3.20	0.17	0.19
ΣE_{tors}	0.17	1.09	0.52	0.21	0.17	0.14	0.14	0.14	0.23	0.21
E_{steric} (total)	1.88	6.27	6.08	7.98	8.42	8.73	8.81	8.16	4.88	4.87

[a] See Figure 4 for numbering scheme. [b] See Table IV. [c] Transition state. [d] $\Sigma E_{vdw} = \Sigma E_{nb} + \Sigma E_{EPR}$.

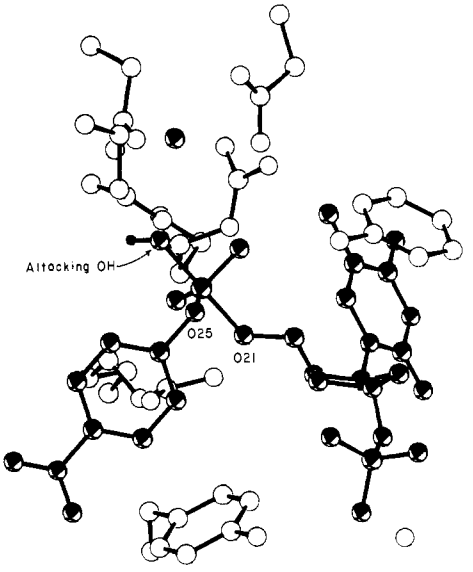

Figure 10. ORTEP drawing of path 2 transition state in hydrolysis of p-NO_2Ph–pdTp in the staphylococcal nuclease environment. Attacking OH is opposite O_{21}–ribose (See Figure 1). Phosphorus bond angles for the transition state are given in Table VI, column 7. Path 2 is of lower energy than path 1 in the enzyme environment. Open circles designate atoms of enzyme; shaded circles, atoms of p-NO_2Ph–pdTp substrate. Orientation of drawing is the same as Figure 3.

The following modifications were performed to obtain a minimum energy structure of thymidine 3′-phosphate 5′-(p-nitrophenyl phosphate). The numbering scheme used is the same as the one used in the pdTp portion of Figure 4. The 3′-phosphate group was added to the ribose ring (atoms 16–20) and the pdTp structure was minimized. (See Table III, column 5, for structural parameters of the minimum energy structure.) The p-nitrophenyl group was added to the 5′-phosphate at oxygen atom, O_{25}. This group was rotated about the P_{22}–O_{25} bond to find a minimum energy conformation. The energy profile showed that a conformation with a torsional angle for $O_{21}P_{22}O_{25}C_{Ph}$ of approximately 30° was one of minimum energy. A similar minimization operation was

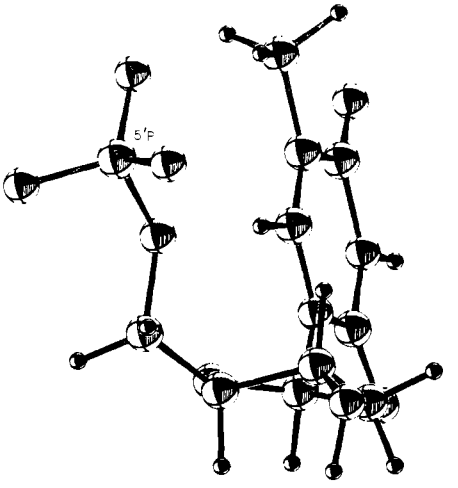

Figure 11. ORTEP drawing of thymidylate ion based on X-ray coordinates of calcium thymidylate.[26]

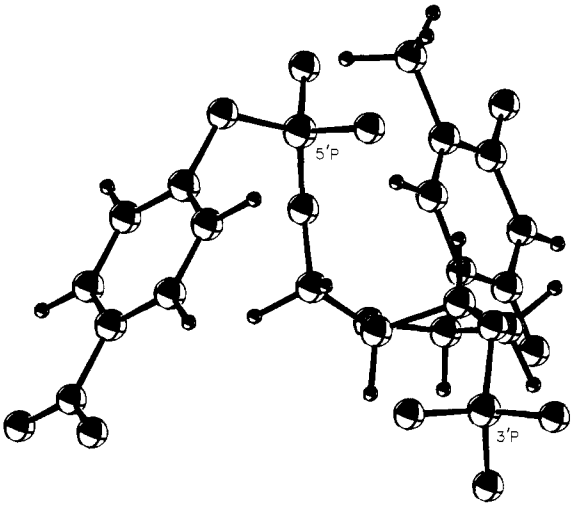

Figure 12. ORTEP drawing of p-NO_2Ph–pdTp based on coordinates obtained from energy minimization with no enzyme constrains (same orientation as Figure 3).

(26) Trueblood, K. N.; Horn, P.; Luzzati, V. *Acta Crystallogr.* **1961**, *14*, 965.

Table VI. Reaction Path 2 for *p*-NO_2Ph-pdTp–Enzyme System (Attacking Group Is OH; Leaving Group Is O_{21}[a])

	point on pathway[b]									
	1	2	3	4	5	6	7[c]	8	9	10
					Bond Length, Å					
P-OH	6.15	3.03	2.55	2.05	1.94	1.84	1.82	1.73	1.61	1.60
P-O_{21}	1.60	1.61	1.62	1.69	1.74	1.80	1.82	1.96	2.97	2.97
P-O_{25}	1.60	1.60	1.60	1.60	1.60	1.61	1.61	1.61	1.60	1.60
P-O_{23}	1.50	1.50	1.50	1.50	1.50	1.50	1.50	1.50	1.50	1.50
P-O_{24}	1.50	1.50	1.50	1.50	1.50	1.50	1.50	1.50	1.50	1.50
					Angle, deg					
$O_{21}PO_{23}$	113.9	110.3	106.9	100.1	98.0	95.4	94.9	91.1	75.7	75.5
$O_{21}PO_{24}$	109.7	105.1	98.7	89.1	86.6	83.8	83.2	79.6	63.7	63.5
$O_{21}PO_{25}$	103.0	106.4	103.8	97.1	95.3	93.0	92.5	88.7	79.3	79.6
O_{21}-P-OH	179.1	178.4	178.8	179.4	179.5	179.6	179.6	179.6	178.5	178.5
$O_{23}PO_{24}$	108.9	112.3	116.1	119.8	120.2	120.3	120.3	120.0	111.8	111.8
$O_{23}PO_{25}$	104.6	103.1	105.4	109.8	110.4	110.7	110.7	110.1	102.7	102.7
O_{23}P-OH	65.6	70.6	73.7	79.8	81.9	84.4	84.9	88.6	104.3	104.5
O_{24}P-O_{25}	116.7	119.4	123.8	128.0	128.7	129.0	128.9	128.5	119.1	119.0
O_{24}P-OH	70.0	73.3	80.1	90.4	93.1	96.1	96.7	100.3	115.1	115.3
O_{25}P-OH	77.8	74.5	77.0	83.6	85.3	87.5	87.9	91.7	102.1	101.9
					Energy, kcal/mol					
ΣE_{str}	0.94	1.05	0.98	1.25	1.30	1.33	1.34	1.23	0.89	0.89
ΣE_{bend}	3.70	4.35	3.99	3.75	3.75	3.75	3.74	3.69	4.05	4.06
ΣE_{VDW}[d]	−2.98	−2.23	−1.26	0.68	1.11	1.45	1.54	1.11	−1.66	−1.64
ΣE_{tors}	0.08	0.10	0.09	0.09	0.08	0.08	0.08	0.08	0.07	0.07
E_{steric} (total)	1.74	3.27	3.80	5.77	6.24	6.61	6.70	6.11	3.35	3.38

[a] See Figure 4 for numbering scheme. [b] See Table IV. [c] Transition state. [d] $\Sigma E_{VDW} = \Sigma E_{nB} + \Sigma E_{EPR}$.

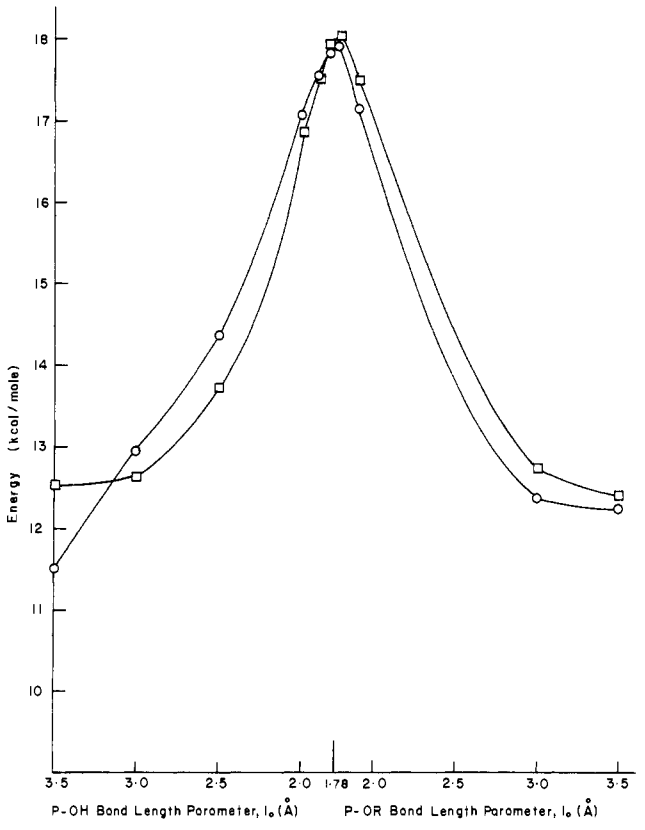

Figure 13. Energy profile for two alternate modes of hydrolysis of *p*-NO_2Ph-pdTp with no enzyme constraints. Circles indicate path 1; squares, path 2. See Figure 1 for definition of pathways. The attacking group is OH and leaving group is OR (OR = O_{25}–Ph in path 1 and O_{21}–ribose in path 2). Experimentally, path 1 is the preferred path in a nonenzymatic environment.

carried out by rotating the phenyl group about the O_{25}–C_{Ph} bond. Like that observed for the enzyme–substrate calculation, the $P_{22}O_{25}C_{Ph}C_{Ph}$ angle always comes back to approximately 90° as the minimum energy conformation, no matter what was taken as the initial angle of rotation. Figures 7 and 12 show the difference in the phenyl ring orientation in the enzyme system as compared to that in the nonenzyme system.

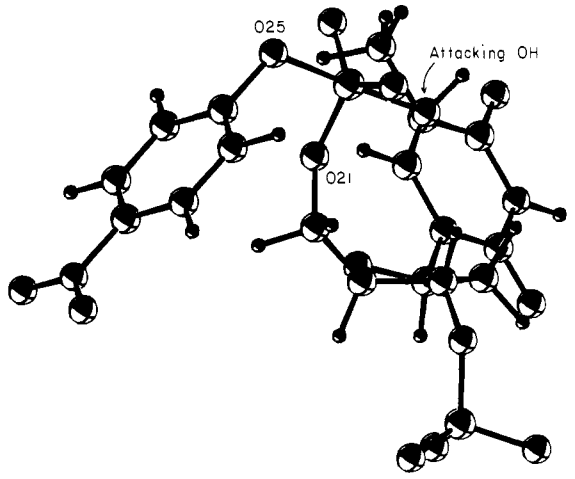

Figure 14. ORTEP drawing of path 1 transition state in hydrolysis of *p*-NO_2Ph-pdTp with no enzyme constraints. Attacking OH is opposite O_{25}–Ph. See Figure 1. Paths 1 and 2 are of similar steric energy in the nonenzyme environment. Orientation of drawing is the same as Figure 3. Phosphorus bond angles for the transition state are given in Table VII, col 7.

The resulting conformation of *p*-NO_2Ph-pdTp, which was used as the ground-state structure for simulation of the nonenzymatic hydrolysis reaction, is shown in Figure 12. Several significant conformational parameters are listed in Table III. Table III and a comparison of Figures 11 and 12 show that the addition of the *p*-nitrophenyl group does not appreciably alter the conformation of the thymidylate structure as determined by the X-ray study.[26]

Under the conditions described in a previous section for reaction pathway calculations, paths 1 and 2 (Figure 1) were investigated by energy minimization at each of 10 points. No atoms were constrained during the energy minimizations.

The results are given in Tables VII and VIII for paths 1 and 2, respectively. The relative energy profile for these two paths is graphed in Figure 13 and ORTEP plots of the transition-state structures are given in Figures 14 and 15.

Discussion

Computer simulation of the two reaction pathways illustrated in Figure 1, under the conditions described herein, reveals that

Table VII. Reaction Path 1 for p-NO_2Ph-pdTp (Nonenzyme System) (Attacking Group Is OH; Leaving Group Is O_{25}[a])

	point on pathway[b]									
	1	2	3	4	5	6	7[c]	8	9	10
					Bond Length, Å					
P-OH	7.55	3.06	2.58	2.05	1.95	1.84	1.82	1.73	1.61	1.60
P-O_{25}	1.60	1.61	1.63	1.70	1.74	1.81	1.82	1.97	3.03	3.22
P-O_{21}	1.60	1.61	1.61	1.61	1.61	1.61	1.61	1.61	1.60	1.60
P-O_{23}	1.50	1.50	1.50	1.50	1.50	1.50	1.50	1.50	1.50	1.50
P-O_{24}	1.50	1.50	1.50	1.50	1.50	1.50	1.50	1.50	1.50	1.50
					Angle, deg					
$O_{21}PO_{23}$	102.8	104.2	107.0	108.1	108.0	107.7	107.7	107.9	104.6	103.9
$O_{21}PO_{24}$	110.7	107.1	113.7	121.2	122.1	122.7	122.8	122.9	118.4	117.9
$O_{21}PO_{25}$	119.3	123.5	116.4	106.5	104.1	101.3	100.8	97.1	80.0	78.2
O_{21}-P-(OH)	61.2	58.9	65.9	75.6	77.9	80.6	81.1	84.6	100.6	102.3
$O_{23}PO_{24}$	110.4	114.5	118.6	126.6	128.2	129.3	129.5	128.6	112.5	110.3
$O_{23}PO_{25}$	105.8	103.1	98.0	91.4	89.2	86.7	86.2	82.9	66.5	64.2
O_{23}P-(OH)	73.6	75.1	80.3	87.0	89.3	91.9	92.4	95.9	113.1	115.5
$O_{24}PO_{25}$	107.4	105.0	102.4	93.3	90.9	88.3	87.7	84.2	72.6	72.8
O_{24}P(OH)	72.6	74.5	77.0	86.3	88.7	91.4	91.9	95.5	107.3	107.0
O_{25}P(OH)	179.4	177.5	177.5	177.7	177.8	177.9	178.0	178.2	179.4	179.5
					Energy, kcal/mol					
ΣE_{str}	0.94	1.11	1.28	1.49	1.51	1.54	1.55	1.50	1.08	1.06
ΣE_{bend}	3.38	3.11	3.27	3.52	3.55	3.55	3.55	3.47	3.16	3.14
ΣE_{VDW}[d]	7.13	8.71	9.77	12.06	12.48	12.74	12.82	12.16	8.12	8.02
ΣE_{tors}	0.03	0.02	0.03	0.03	0.03	0.02	0.02	0.02	0.02	0.03
E_{steric} (total)	11.48	12.95	14.35	17.10	17.57	17.85	17.94	17.15	12.38	12.25

[a] See Figure 4 for numbering scheme. [b] See Table IV. [c] Transition state. [d] $\Sigma E_{VDW} = {}^2\Sigma E_{nB} + \Sigma E_{EPR}$.

Table VIII. Reaction Path 2 for p-NO_2Ph–pdTp (Nonenzyme System) (Attacking Group Is OH; Leaving Group Is O_{21}[a])

	point on pathway[b]									
	1	2	3	4	5	6	7[c]	8	9	10
					Bond Length, Å					
P(OH)	9.64	3.05	2.58	2.06	1.95	1.84	1.82	1.73	1.61	1.60
PO_{21}	1.60	1.61	1.63	1.70	1.74	1.81	1.82	1.97	3.04	3.33
PO_{23}	1.50	1.50	1.50	1.50	1.50	1.50	1.50	1.50	1.50	1.50
PO_{24}	1.50	1.50	1.50	1.50	1.50	1.50	1.50	1.50	1.50	1.50
PO_{25}	1.60	1.60	1.60	1.60	1.61	1.61	1.61	1.61	1.60	1.60
					Angle, deg					
$O_{21}PO_{23}$	102.6	102.1	99.8	93.3	91.3	88.9	88.5	85.1	70.8	69.7
$O_{21}PO_{24}$	111.4	110.5	106.4	98.0	95.8	93.1	92.6	89.2	70.6	67.3
$O_{21}PO_{25}$	119.1	115.2	109.1	100.3	98.2	95.7	95.2	92.2	85.1	84.8
O_{21}P(OH)	180.0	179.9	179.6	179.2	179.1	179.0	179.0	178.9	179.1	179.1
$O_{23}PO_{24}$	110.0	110.5	111.5	111.4	111.3	111.0	110.8	110.9	109.6	108.3
$O_{23}PO_{25}$	105.7	106.7	108.1	108.0	107.9	107.6	107.4	107.6	108.1	107.3
O_{23}P(OH)	77.4	77.9	79.9	85.9	87.8	90.1	90.5	93.8	108.5	109.7
$O_{24}PO_{25}$	107.6	111.4	120.1	135.0	137.9	140.6	141.1	141.5	124.2	122.2
O_{24}P(OH)	68.6	69.4	73.6	82.2	84.5	87.2	87.7	91.2	109.3	112.3
O_{25}P(OH)	60.9	64.9	71.2	80.0	82.2	84.6	85.1	88.2	95.7	96.1
					Energy, kcal/mol					
ΣE_{str}	0.95	0.99	1.17	1.45	1.49	1.52	1.53	1.48	1.03	0.98
ΣE_{bend}	3.38	3.33	3.48	3.77	3.83	3.89	3.90	3.86	3.35	3.33
ΣE_{VDW}[d]	8.18	8.26	9.20	11.66	12.17	12.55	12.66	12.13	8.30	8.09
ΣE_{tors}	0.04	0.03	0.03	0.03	0.03	0.03	0.03	0.03	0.03	0.03
E_{steric} (total)	12.55	12.61	13.88	16.91	17.52	17.99	18.12	17.50	12.71	12.43

[a] See Figure 4 for numbering scheme. [b] See Table IV. [c] Transition state. [d] $\Sigma E_{VDW} = \Sigma E_{nB} + \Sigma E_{EPR}$.

the activation energy for paths 1 and 2 for the nonenzyme hydrolysis of p-NO_2Ph–pdTp (Figure 13) is comparable, near 6 kcal/mol. Significantly, however, Figure 8 for these two paths for staphylococcal nuclease action on the same substrate shows the activation energy for path 1 to be approximately 2 kcal higher than that for path 2. The lower energy obtained for path 2 is consistent with kinetic studies[8] giving exclusive formation of p-nitrophenyl phosphate and thymidine 3′-phosphate. The higher activation energies for path 1 of the enzymatic hydrolysis relative to the three other pathways is attributable, for the most part, to higher van der Waals interactions in the transition states for this pathway; cf. Tables VI, VII, and VIII with Table V.

As depicted in Figures 7 and 12, the substrate geometry established in the simulation process as the ground state differs considerably for the enzyme and nonenzyme systems. (See also Table III.) The different substrate conformations are directly related to the type of enzyme constraints chosen in this study. The results suggest a reasonable validity for their importance in the actual enzyme system.

As seen for the transition states shown in Figures 9 and 10 for paths 1 and 2, respectively, for the enzyme hydrolysis, in-line attack does not drastically alter the general substrate conformation except in the immediate vicinity of the 5′-phosphate unit. The same is true for the nonenzymatic routes, which, in these cases, lack enzyme constraints. Hence, it might be surmised that enzyme constraints are effective in choosing the most effective geometry for nucleophilic attack that leads to a low energy profile for efficient catalysis.

Although it is not apparent that in the enzyme system in-line OH attack opposite the better leaving group, p-nitrophenoxide

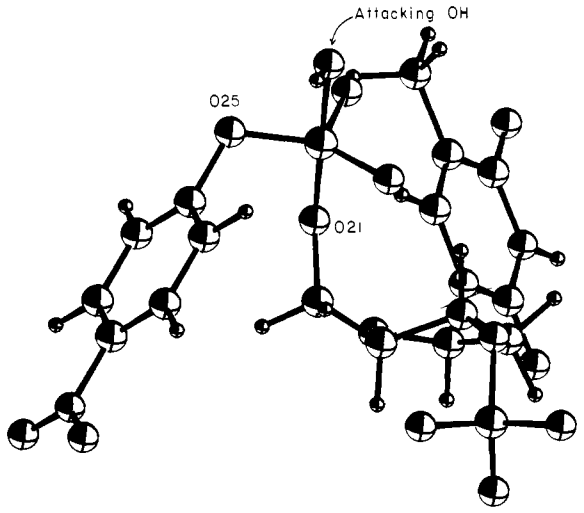

Figure 15. ORTEP drawing of path 2 transition state in hydrolysis of p-NO_2Ph–pdTp with no enzyme constraints. Attacking OH is opposite O_{21}–ribose. See Figure 1. Paths 1 and 2 are of similar steric energy in the nonenzymatic environment. Orientation of drawing is the same as Figure 3. Phosphorus bond angles for the transition state are given in Table VIII, column 7.

(path 1), will give a transition state of higher energy than that for path 2, the increased steric interactions associated with path 1 (Table V) imply a poorer fit between enzyme residues and the transition-state geometry.

Of course, the condition on both the enzyme and nonenzyme hydrolysis pathways requiring the bending force constant, k_b, to be sufficiently large [(1 mdyn Å)/rad^2] to hold the attacking OH group and leaving group in-line assures that a transition state will form with these groups axially oriented in an approximately trigonal-bipyramidal geometry. This is a reasonable condition in this case. On the basis of known phosphorane compound studied by X-ray diffraction,[9] derivatives with acyclic substituents attached to phosphorus have structures that do not deviate much from an idealized trigonal bipyramid.[27] Use of an increasing number of five-membered cyclic substitutents at phosphorus, especially with ring unsaturation, results in structural changes toward a square pyramid.[27] In the simulation of RNase action on UpA,[4] we set this bending force constant to zero in accord with the formation of a cyclic intermediate. This resulted in a transition-state geometry intermediate between the trigonal bipyramid and square pyramid.[28]

The fact that axial bonds are weaker than equatorial bonds for a trigonal bipyramid[29] is the principal reason why entering and leaving groups are postulated to do so from these positions.[30] Even though the nonenzyme paths are not differentiated by their activation energies based on strain considerations (Figure 13), path 1 is favored in terms of bonding considerations, leading to the release of thee better departing group. path 1 is the nonenzymatically observed route.[8]

Other R groups attached to the 5′-phosphate allow efficient catalysis, e.g., p-aminophenyl or a methyl group.[7,25] A modest size change does not seem to be a factor. The p-nitrophenyl group when attached to the pdTp substrate minimized with no appreciable buildup of steric strain. Presumably other R groups would result in a similar active substrate geometry (cf. Figure 7).

We are not able to differentiate between degrees of substrate activity with the present type of calculation. On going from the inactive substrate, pdTp, to an active one, R–pdTp, the 5′-phosphate goes from a dianionic species to the monoanionic diester form. It may be possible to make the four hydrogen bonding force constants between the 5′-phosphate oxygen atooms and the Arg-35 and Arg-87 residues (Figure 5) larger for the dianionic form to hold it in a more rigid position and, thus, mimic substrate activity by a resultant increase in strain terms on hydrolysis. Electronically, the dianion is less subject to nucleophilic attack.

Similarly, one may mimic changes in base specificity, i.e., A and T nucleotidyl portions hydrolyze faster than C- and G-containing substrates, or changes in metal ion.[7] Group 2B divalent metal ions competitively inhibit staphylococcal nuclease activity.[31] All of these factors suggest the extremely delicate balance of electronic and steric interactions at an active site that make an enzyme operate so effectively compared to nonenzyme routes. Further, complementation studies indicate that almost the entire amino acid sequence is needed for the maintenance of nuclease activity.[7]

Rather than the in-line mechanism considered here, one might consider the possibility of an adjacent process, whereby the incoming group enters an axial position adjacent to the leaving group (equatorially situated). In this process, ligand exchange occurs (pseudorotation) during the lifetime of the transition state to bring the group undergoing hydrolysis to a departing axial position.[30] We simulated the adjacent mechanism in the RNase system[4] and found high barriers for potential pseudorotational processes. The same arguments given there apply here. In general, we see no valid reason for expecting an enzyme system to accommodate a facile intramolecular ligand exchange process.

On the basis of 1.5-Å X-ray data, Tucker, Hazen, and Cotton[11] have proposed an active-site geometry for staphylococcal nuclease–pdTp–Ca(II), which differs somewhat from the active site used in this calculation based on 2.0-Å data. We have carried out preliminary calculations of reaction pathways based on 1.5-Å data that incorporate the new features of the active site[11] and retain calculation conditions as described in this paper. These calculations show that the mechanism proposed by Tucker, Hazen, and Cotton[11] is sterically reasonable and the energy profile for path 1 and path 2 in the enzyme environment is similar to that shown in Figure 8 for 2.0-Å data.

Acknowledgments. This investigation was suported by a grant from the National Institutes of Health (GM 21466) and is gratefully acknowledged. Appreciation is expressed to the University of Massachusetts Computing Center for generous allocation of computer time.

Registry No. (p-NO_2Ph-pdTp), 24418-11-9; (pdTp), 2863-04-9; tyr, 60-18-4; lys, 56-87-1; glu, 56-86-0; asp, 56-84-8; calcium, 7440-70-2; staphylococcal nuclease, 9013-53-0.

(27) (a) Holmes, R. R.; Deiters, J. A. *J. Am. Chem. Soc.* **1977**, *99*, 3318. (b) Holmes, R. R. *Acc. Chem. Res.* **1979**, *12*, 257.
(28) See also: Holmes, R. R. *Int. J. Pept. Protein Res.* **1976**, *8*, 445.
(29) Holmes, R. R. *Acc. Chem. Res.* **1972**, *5*, 296.
(30) Westheimer, F. H. *Acc. Chem. Res.* **1968**, *1*, 70.
(31) Cuatrecasas, P.; Fuchs, S.; Anfinsen, C. B. *J. Biol. Chem.* **1967**, *242*, 1541.